Synthesis and Functional Properties of Donor−Acceptor π-Conjugated Oligomers

ARTICLE *in* CHEMISTRY OF MATERIALS · MARCH 2003

Impact Factor: 8.35 · DOI: 10.1021/cm0208915

4 AUTHORS, INCLUDING:

Zhong Hui Li,
Chengdu Normal University
36 PUBLICATIONS **863** CITATIONS
SEE PROFILE

Marie D'Iorio
National Research Council Canada
95 PUBLICATIONS **3,020** CITATIONS
SEE PROFILE

Synthesis and Functional Properties of Donor−Acceptor π-Conjugated Oligomers

Man Shing Wong,*,† Zhong Hui Li,† Ye Tao,‡ and Marie D'Iorio‡

Department of Chemistry, Hong Kong Baptist University, Kowloon Tong, Hong Kong, SAR China, and Institute for Microstructural Sciences, National Research Council of Canada, M-50 Montreal Road, Ottawa, Ontario, Canada, K1A 0R6

Received September 4, 2002. Revised Manuscript Received December 18, 2002

Novel donor−acceptor oligophenylenevinylenes (OPVs) bearing an electron-donating 2-(2-butoxyethoxy)ethoxy group at one end and various electron-withdrawing groups including alkylsulfonyl, cyano, and nitro functionalities at the other end have been synthesized for investigation of structure−functional property relationships. Depending on the nature of the electron-withdrawing group, the newly synthesized donor−acceptor OPVs can exhibit an efficient light-emitting property or a large photovoltaic effect. The asymmetrically disubstituted OPV bearing 2-(2-butoxy-ethoxy)ethoxy-hexylsulfonyl functionalities possesses superior molecular properties for light-emitting applications than the symmetrically 2-(2-butoxyethoxy)ethoxy-disubstituted counterparts. In addition, our first observation and investigation on the photovoltaic response in polyalkyleneoxy-nitro disubstituted OPV series is reported. The spectral responsivity of the photovoltaic device corresponds to the absorption characteristics of the oligomer. Most importantly, the photocurrent responsivity increases with an extension of the conjugated length of the oligomer.

Introduction

Molecular semiconducting materials have been extensively explored and investigated for various technologically functional properties for next-generation electronic and optoelectronic applications[1] such as electroluminescent devices,[2−4] field-effect transistors,[5−7] photovoltaic devices,[8,9] electro-optic modulators,[10] and solid-state lasers[11] in the past decade. In addition to polymeric materials, the use of functionalized π-conjugated molecules and oligomers as an active component in device applications such as a light-emitting layer in an organic light-emitting diode (LED)[12] and a p-type semiconductor in a field-effect transistor[7,13] has recently received considerable attention since these can exhibit unique and interesting optoelectronic properties. As a result, over the past few years, a wide range of functionalized π-conjugated molecules and oligomers have been designed and synthesized to tune the desirable (non)-optical and electronic properties and to enhance the processing and morphological properties of the functional materials.[14−18] Furthermore, the monodispersed, well-defined π-conjugated oligomers can serve as model compounds for understanding the fundamental properties of the related polymers.[19,20] The design of useful molecular materials requires understanding and optimization of the functional properties of a molecule. However, subtle modifications of the functional part of π-conjugated molecules often leads to a dramatic change in the optical, electronic, or processing properties of a material. Therefore, knowledge of structure−functional property relationships is essential toward a rational design and optimization of functional organic and polymeric materials.

In the past few years, we have been investigating the effect of the surface-functionalized dendritic wedges on light-emitting properties of dendrimers[21] and the influence of substitution and chain-length effect on various

* To whom correspondence should be addressed.
† Hong Kong Baptist University.
‡ National Research Council of Canada.

(1) Sheats, J. R.; Barbara, P. F. *Acc. Chem. Res.* **1999**, *32*, 191−192.
(2) Kraft, A.; Grimsdale, A. C.; Holmes, A. B. *Angew. Chem., Int. Ed.* **1998**, *37*, 402−428.
(3) Friend, R. H.; Gymer, R. W.; Holmes, A. B.; Burroughes, J. H.; Marks, R. N.; Taliani, C.; Bradley, D. D. C.; Dos Santos, D. A.; Brédas, J. L.; Lögdlund, M.; Salaneck, W. R. *Nature* **1999**, *397*, 121−128.
(4) Mitschke, U.; Bäuerle, P. *J. Mater. Chem.* **2000**, *10*, 1471−1507.
(5) Katz, H. E. *J. Mater. Chem.* **1997**, *7*, 369−376.
(6) Horowitz, G. *Adv. Mater.* **1998**, *10*, 365−377.
(7) Garnier, F. *Acc. Chem. Res.* **1999**, *32*, 209−215.
(8) Sariciftci, N. S.; J., H. A. *Photophysics, Charge Separation and Device Applications of Conjugated Polymer/Fullerene Composites*; Nalwa, H. S., Ed.; John Wiley & Sons Ltd.: New York, 1997; Vol. 1, pp 414−455.
(9) Brabec, C. J.; Sariciftci, N. S.; Hummelen, J. C. *Adv. Funct. Mater.* **2001**, *11*, 15−26.
(10) Marder, S. R.; Kippelen, B.; Jen, A. K. Y.; Peyghambarian, N. *Nature* **1997**, *388*, 845−851.
(11) Hide, F.; Diaz-Garcia, M. A.; Schwartz, B. J.; Heeger, A. I. *Acc. Chem. Res.* **1997**, *30*, 430−436.
(12) Chan, L. H.; Lee, R. H.; Hsieh, C. F.; Yeh, H. C.; Chen, C. T. *J. Am. Chem. Soc.* **2002**, *124*, 6469−6479, and references therein.
(13) Garnier, F.; Hajlaoui, R.; Yassar, A. *Sciences* **1994**, *265*, 1684.
(14) Tour, J. M. *Chem. Rev.* **1996**, *96*, 537−553.
(15) Berresheim, A. J.; Müller, M.; Müllen, K. *Chem. Rev.* **1999**, *99*, 1747−1785.
(16) Segura, J. L.; Martin, N. *J. Mater. Chem.* **2000**, *10*, 2403−2453.
(17) Shirota, Y. *J. Mater. Chem.* **2000**, *10*, 1−25.
(18) Bunz, U. H. F. *Chem. Rev.* **2000**, *100*, 1605−1644.
(19) Müllen, K.; Wegner, G. *Electronic Materials: The Oligomer Approach*; Wiley-VCH: Weinheim, 1998.
(20) Martin, R. E.; Diederich, F. *Angew. Chem., Int. Ed.* **1999**, *38*, 1350−1377.
(21) (a) Kwok, C. C.; Wong, M. S. *Macromolecules* **2001**, *34*, 6821−6830. (b) Kwok, C. C.; Wong, M. S. *Chem. Mater.* **2002**, *14*, 3156−3166.

10.1021/cm0208915 CCC: $25.00
Published on Web 02/12/2003

functional properties of soluble and highly coplanar end-functionalized oligophenylenevinylenes (OPVs). We have previously shown that highly luminescent, multialkoxy end-functionalized OPVs show potential for light-emitting applications,[22] hexylsulfanyl end-substituted OPVs selectively respond to Ag^+ ion in membrane optode sensors,[23] and highly coplanar OPVs with a long conjugated length exhibit very large third-order optical nonlinearities.[24] Continuing our effort to probe the structural factors that can enhance a specific functional property of a molecule (or material), we herein report the synthesis and investigation of the structure−functional property relationship of novel donor−acceptor π-conjugated oligomers, OPV. Although donor−acceptor π-conjugated molecules have been widely studied for second-order nonlinear optical properties in the past decades,[25] there are only a few studies on other functional properties.[26−28] The influence of the electron-withdrawing group of donor−acceptor OPVs (**1**−**3**) on various molecular properties was first investigated. Depending on the nature of the electron-withdrawing substituent, the newly synthesized OPVs can exhibit either an efficient light-emitting property or a large photovoltaic effect. In addition, the structure−photovoltaic property of alkoxy-nitro disubstituted oligomers/molecules (**3**−**5**, **17**, and **18**) was explored.

Experimental Section

^{1}H NMR spectra were recorded using either a JEOL JHM-EX270 FT NMR spectrometer or a Varian INOVA-400 FT NMR spectrometer and are referenced to the residual $CHCl_3$ peak at 7.24 ppm. ^{13}C NMR spectra were recorded using a Varian INOVA-400 FT NMR spectrometer and are referenced to the $CDCl_3$ peak at 77 ppm. All the spectroscopic measurements were performed in $CHCl_3$. Electronic absorption (UV−vis) and fluorescence spectra were recorded using a Varian Cary 100 Scan Spectrophotometer and a PTI Luminescence Spectrophotometer, respectively. The fluorescence quantum yields in chloroform using 9,10-diphenylanthrancene as a standard were determined by the dilution method as described by Parker and Rees.[29] The organic light-emitting diodes and photovoltaic devices were prepared on commercial ITO-coated glass substrates (Applied Films Corp.) with a sheet resistance of 12 Ω/m^2 and an ITO thickness of ∼120 nm. Before lithographic patterning, the ITO substrates were cleaned using cleanroom soap, acetone, and 2-propanol. The anodes were formed by etching the patterned ITO substrates in a solution of $HCl:HNO_3:H_2O$ (25:2:25). The patterned ITO substrates were treated in a UV ozone oven for 10 min before being loaded into the vacuum chamber. The LED device structures consisted of 50-nm TPD as a hole transport layer, 50-nm OPV as an emissive layer, 20-nm PBD or 2-nm LiF as a hole-blocking layer, and thermally evaporated aluminum and silver layer as a cathode. All depositions were performed at high vacuum (2×10^{-7} Torr). A typical growth rate of 2 Å/s was used and the substrates was held at room temperature. The active device area is 1.0×5.0 mm^2. The devices were operated and characterized at ambient temperature. The EL spectra and luminance were measured by using a Photo Research-650 SpectraColorimeter, and the current−voltage ($I-V$) characteristics were measured with a Keithley 236 source measure unit. A typical photovoltaic cell consists of 40-nm TPD as a hole transport layer, 40-nm photovoltaic material as an active layer, and 150-nm Al and 50-nm Ag layer as a cathode. In some of the photovoltaic devices, the photovoltaic layer was made by co-evaporation of Alq_3 and OPV at a 100:5 ratio. All of these devices were also operated and characterized in air.

The general procedure for the Wadsworth−Emmon reactions reported previously was followed.[24,30]

1. ^{1}H NMR (300 MHz, $CDCl_3$, δ): 7.85 (d, J = 8.49 Hz, 2H), 7.64 (d, J = 8.52 Hz, 2H), 7.49 (s, 4H), 7.43 (d, J = 8.79 Hz, 2H), 7.23 (d, J = 16.38 Hz, 1H), 7.10 (d, J = 16.41 Hz, 1H), 7.09 (d, J = 16.41 Hz, 1H), 6.95 (d, J = 16.26 Hz, 1H), 6.90 (d, J = 8.79 Hz, 2H), 4.14 (t, J = 4.92 Hz, 2H), 3.86 (t, J = 4.94 Hz, 2H), 3.71 (m, 2H), 3.59 (m, 2H), 3.46 (t, J = 6.72 Hz, 2H), 3.07 (t, J = 8.10 Hz, 2H), 1.70 (m, 2H), 1.56 (m, 2H), 1.33 (m, 4H), 1.24 (m, 4H), 0.90 (t, J = 7.35 Hz, 3H), 0.84 (t, J = 6.87 Hz, 3H). ^{13}C NMR (100 MHz, $CDCl_3$, δ): 158.7, 142.8, 138.1, 137.3, 135.1, 132.2, 130.0, 128.8, 128.5, 127.8, 127.3, 126.9, 126.6, 126.1, 125.9, 114.9, 71.2, 70.9, 70.1, 69.7, 67.5, 56.4, 31.7, 31.1, 29.7, 27.9, 22.6, 22.3, 19.2, 13.9. MS (EI) m/z: 590.2 (M^+). HRMS (EI): calcd for $C_{36}H_{46}O_5S$, 590.3066; found, 590.3077. Anal. Calcd for $C_{36}H_{46}O_5S$: C, 73.19; H, 7.85; S, 5.43. Found: C, 73.20; H, 8.12; S, 5.16. mp: 216−217 °C.

2. ^{1}H NMR (400 MHz, $CDCl_3$, δ): 7.61 (d, J = 8.4 Hz, 2H), 7.56 (d, J = 8.0 Hz, 2H), 7.48 (s, 4H), 7.43 (d, J = 8.4 Hz, 2H), 7.19 (d, J = 16.4 Hz, 1H), 7.08 (d, J = 16.0 Hz, 1H), 7.06 (d, J = 16.4 Hz, 1H), 6.95 (d, J = 16.0 Hz, 1H), 6.90 (d, J = 8.4 Hz, 2H), 4.14 (t, J = 4.8 Hz, 2H), 3.86 (t, J = 4.8 Hz, 2H), 3.71 (m, 2H), 3.60 (m, 2H), 3.46 (t, J = 6.6 Hz, 2H), 1.56 (m, 2H), 1.34 (m, 2H), 0.90 (t, J = 7.4 Hz, 3H). ^{13}C NMR (100 MHz, $CDCl_3$, δ): 158.7, 141.9, 138.1, 135.1, 132.5, 132.0, 130.0, 128.8, 127.8, 127.3, 126.8, 126.6, 126.2, 125.9, 119.1, 114.9, 110.4, 71.2, 70.9, 70.1, 69.7, 67.5, 31.7, 19.3, 13.9. MS (FAB) m/z: 467.5 (M^+). Anal. Calcd for $C_{31}H_{33}NO_3$: C, 79.63; H, 7.11; N, 2.00. Found: C, 79.48; H, 7.21; N, 2.01. mp: 230−232 °C.

3. ^{1}H NMR (270 MHz, $CDCl_3$, δ): 8.22 (d, J = 8.91 Hz, 2H), 7.63 (d, J = 8.91 Hz, 2H), 7.52 (s, 4H), 7.45 (d, J = 8.91 Hz, 2H), 7.26 (d, J = 16.47 Hz, 1H), 7.14 (d, J = 16.2 Hz, 1H), 6.97 (d, J = 16.74 Hz, 1H), 6.92 (d, J = 8.64 Hz, 2H), 4.17 (t, J = 4.86 Hz, 2H), 3.88 (t, J = 4.86 Hz, 2H), 3.73 (m, 2H), 3.62 (m, 2H), 3.48 (t, J = 6.62 Hz, 2H), 1.58 (m, 2H), 1.37 (m, 2H), 0.92 (t, J = 7.29 Hz, 3H). ^{13}C NMR (100 MHz, $CDCl_3$, δ): 158.7, 146.6, 143.9, 138.3, 135.0, 132.9, 130.0, 129.0, 127.8, 127.4, 126.8, 126.7, 125.8, 125.7, 124.1, 114.9, 71.2, 70.9, 70.1, 69.7, 67.5, 31.7, 19.3, 13.9. MS (FAB) m/z: 487.4 (M^+). Anal. Calcd for $C_{30}H_{33}NO_5$: C, 73.89; H, 6.82; N, 2.87. Found: C, 73.97; H, 6.91; N, 2.81. mp: 228 °C.

4. ^{1}H NMR (270 MHz, $CDCl_3$, δ): 8.18 (d, J = 8.91 Hz, 2H), 7.57 (d, J = 8.64 Hz, 2H), 7.46 (d, J = 8.64 Hz, 2H), 7.20 (d, J = 16.2 Hz, 1H), 6.98 (d, J = 16.2 Hz, 1H), 6.92 (d, J = 8.91 Hz, 2H), 4.16 (t, J = 4.86 Hz, 2H), 3.87 (t, J = 4.86 Hz, 2H), 3.71 (m, 2H), 3.61 (m, 2H), 3.46 (t, J = 6.62 Hz, 2H), 1.56 (m, 2H), 1.34 (m, 2H), 0.90 (t, J = 7.29 Hz, 3H). ^{13}C NMR (100 MHz, $CDCl_3$, δ): 159.5, 146.4, 144.3, 132.9, 129.1, 128.4, 126.5, 124.2, 115.0, 71.3, 70.9, 70.1, 69.7, 67.5, 31.7, 19.3, 13.9. MS (FAB) m/z: 385.4 (M^+). HRMS (ESI-TOF): calcd for $C_{22}H_{28}NO_5$, 386.1967; found, 386.1964. mp: 49−51 °C.

5. ^{1}H NMR (270 MHz, $CDCl_3$, δ): 8.21 (d, J = 8.64 Hz, 2H), 7.62 (d, J = 8.64 Hz, 2H), 7.53 (s, 4H), 7.50 (s, 4H), 7.26 (d, J = 15.93 Hz, 1H), 7.14 (d, J = 16.74 Hz, 1H), 7.13 (s, 2H), 7.06 (d, J = 15.93 Hz, 1H), 6.98 (d, J = 16.21 Hz, 1H), 6.72 (s, 2H), 4.16 (t, J = 5.27 Hz, 2H), 3.89 (s, 6H), 3.81 (t, J = 5.27 Hz, 2H), 3.71 (m, 2H), 3.59 (m, 2H), 3.46 (t, J = 6.75 Hz, 2H), 1.56 (m, 2H), 1.35 (m, 2H), 0.90 (t, J = 7.29 Hz, 3H). ^{13}C NMR (100

(22) Wong, M. S.; Li, Z. H.; Shek, M. F.; Chow, K. H.; Tao, Y.; D'Iorio, M. *J. Mater. Chem.* **2000**, *10*, 1805−1810.
(23) Wong, M. S.; Chan, W. H.; Chan, W. Y.; Li, J.; Dan, X. *Tetrahedron Lett.* **2000**, *41*, 9293−9297.
(24) Wong, M. S.; Li, Z. H.; Shek, M. F.; Samoc, M.; Samoc, A.; Luther-Davies, B. *Chem. Mater.* **2002**, *14*, 2999−3004.
(25) Verbiest, T.; Houbrechts, S.; Kauranen, M.; Clays, K.; Persoons, A. *J. Mater. Chem.* **1997**, *7* (11), 2175−2189.
(26) Zhang, X. H.; Chen, B. J.; Lin, X. Q.; Wong, O. Y.; Lee, C. S.; Kwong, H. L.; Lee, S. T.; Wu, S. K. *Chem. Mater.* **2001**, *13*, 1565−1569.
(27) Piechowski, A. P.; Bird, G. R.; Morel, D. L.; Stogryn, E. L. *J. Phys. Chem.* **1984**, *88*, 934−950.
(28) Morel, D. L.; Stogryn, E. L.; Ghoshl, A. K.; Feng, T.; Purwin, P. E.; Shaw, R. F.; Fishman, C.; Piechowski, A. P.; Bird, G. R. *J. Phys. Chem.* **1984**, *88*, 923−933.
(29) Parker, C. A.; Rees, W. T. *Analyst* **1960**, *85*, 587−589.
(30) Wong, M. S.; Samoc, M.; Samoc, A.; Luther-Davies, B.; Humphrey, M. G. *J. Mater. Chem.* **1998**, *8*, 2005−2009.

Scheme 1. Synthesis of Donor−Acceptor Three-Phenyl-Ring OPVs, 1−3

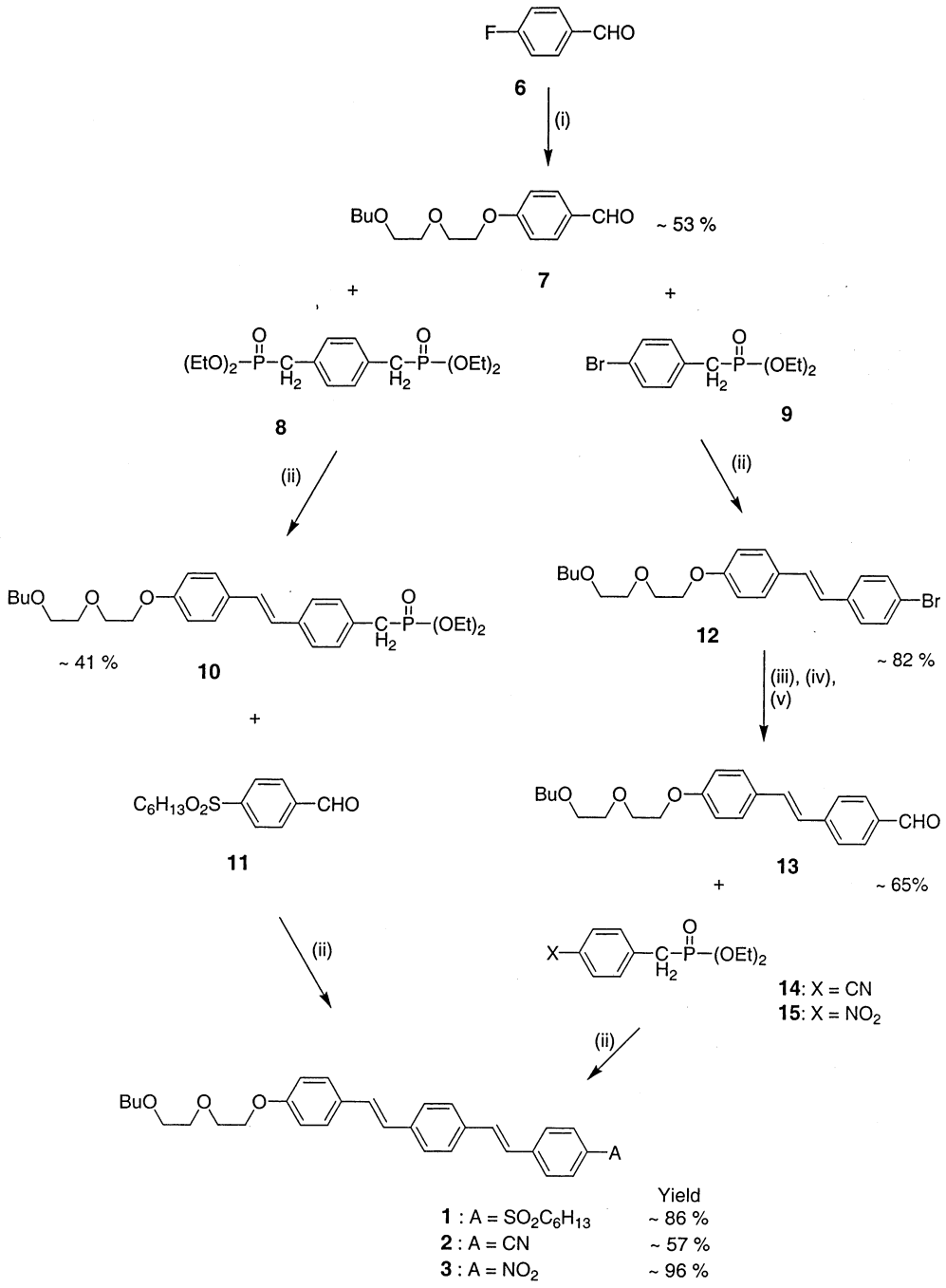

Reagents and Conditions: (i) $BuO(EtO)_2H$, Na_2CO_3, DMSO, N_2, 150-160 °C, overnight; (ii) NaH, DME, 0 °C to rt, 4h; (iii) nBuLi, THF, -78 °C, 2h; (iv) DMF, -78 °C to 0 °C, 1 h; (v) H^+.

MHz, $CDCl_3$, δ): 153.5, 146.7, 143.8, 137.9, 137.1, 136.9, 136.4, 135.4, 133.0, 132.8, 128.9, 128.8, 127.8, 127.6, 127.4, 127.0, 126.8, 126.0, 124.2, 103.7, 72.3, 71.2, 70.6, 70.4, 70.1, 56.1, 31.7, 19.3, 13.9. MS (FAB) *m*/*z*: 649.5 (M^+). Anal. Calcd for $C_{40}H_{43}NO_7$: C, 73.93; H, 6.67: N, 2.15%. Found: C, 74.10; H, 6.80; N, 2.14%. mp: 145 °C (dec).

Results and Discussion

The trans carbon−carbon double bonds of donor−acceptor OPVs were synthesized by the iterative Wadsworth−Emmons reactions using the strategy established previously.[22] To take advantage of commercially available starting materials, we devised two routes to synthesize three-phenyl-ring OPVs **1**−**3** bearing an electron-donating 2-(2-butoxyethoxy)ethoxy group at one end and various electron-withdrawing groups at the other end, which are summarized in Scheme 1. For the first approach, nucleophilic aromatic substitution of 4-fluorobenzaldehyde, **6**, with 2-(2-butoxyethoxy)ethanol in the presence of Na_2CO_3 as a base in DMSO afforded 4-[2-(2-butoxyethoxy)ethoxy]benzaldehyde, **7**. The Mono−Wadsworth−Emmons reaction of bis(diethyl)-*p*-xylylene-(bis(phosphonate)), **8**, with benzaldehyde **7** yielded 4-[2-(2-butoxyethoxy)ethoxy)]styrylbenzylphosphonate, **10**. Subsequent Wadsworth−Emmons reaction of **10** and 4-hexylsulfonylbenzaldehyde, **11**, afforded **1** in a good

Scheme 2. Syntheses of 4,4′-Polyalkyleneoxy-nitro Disubstituted Stilbene, 4, and Four-Phenyl-Ring OPV, 5

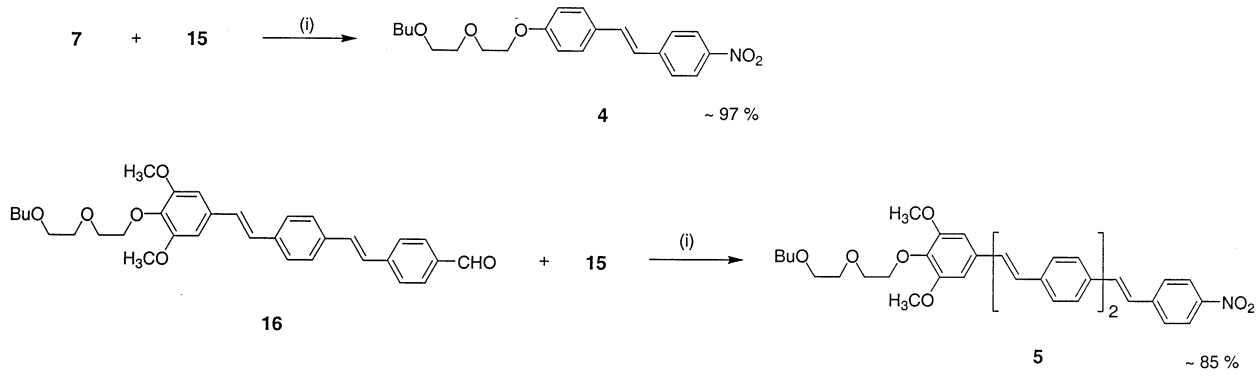

Reagents and Conditions: (i) NaH, DME, 0 °C to rt, 4h

yield (86%). In the second route, the Wadsworth−Emmons reaction of 4-bromobenzylphosphonate ester, **9**, with benzaldehyde **7** yielded 4-bromo-4′-[2-(2-butoxyethoxy)ethoxy]stilbene, **12**. Lithium−halogen exchange of **12** at −78 °C followed by reaction with DMF and then acid hydrolysis yielded 4-[2-(2-butoxyethoxy)ethoxy]-styrylbenzaldehyde, **13**. Subsequent Wadsworth−Emmons reaction of **13** and the corresponding benzylphosphonate ester (**14** or **15**), which was prepared by the Michaelis−Arbuzov reaction of triethyl phosphite and the corresponding benzyl bromide, afforded **2** and **3** in moderate to good yields (57% and 96%), respectively.

On the other hand, syntheses of 4,4′-polyalkyleneoxy-nitro disubstituted stilbene **4** and disubstituted four-phenyl-ring OPV **5** are outlined in Scheme 2. 4-[2-(2-Butoxyethoxy)ethoxy]-4′-nitrostilbene, **4**, was prepared by the Wadsworth−Emmons reaction of **7** and **15**. In a similar fashion, the four-phenyl-ring OPV **5** was synthesized by the reaction of phosphonate **15** and 4-{4-[2-(2-butoxyethoxy)ethoxy]styryl}styrylbenzaldehyde, **16**, which was prepared using procedures published previously. All of the newly synthesized OPVs were fully characterized with standard spectroscopic techniques including ^{1}H NMR, ^{13}C NMR, and low-/high-resolution mass spectroscopy or elemental analysis.

In contrast to symmetrically disubstituted OPVs, the absorption spectra of these donor−acceptor OPVs show no apparent vibronic structures, indicating the dominance of the intramolecular charge-transfer excited state. Consistent with the predicted trend, the donor−acceptor OPVs **1**−**3** exhibit substantial red shift in the absorption maxima relative to the polyalkyleneoxy disubstituted OPV counterparts (λ_{max} = 368 nm). Furthermore, the red shift in their emission spectra (E_{max} for **1** = 478 nm and E_{max} for **2** = 471 nm) is even greater than in the absorption spectra when compared to those of the symmetrically disubstituted OPV (E_{max} = 431 nm). Interestingly, **1** and **2** exhibit a strong fluorescence with fluorescence quantum yields of 64% and 52%, respectively, measured in chloroform, but **3** shows almost no fluorescence in solution.

Multilayer light-emitting devices (LED) using the newly synthesized donor−acceptor OPVs as an emissive layer were fabricated by vacuum deposition and investigated. For both the **1**- and **2**-based devices, the electroluminescence (EL) spectra resemble the corresponding solid-state photoluminescence (PL) spectra and the spectral features are independent of the applied voltage. These consistently suggest that the emission originates from the oligomer. For comparison, the polyalkyleneoxy disubstituted OPV-based LED was also prepared under the same conditions. **1**-based LED exhibits the external EL efficiency of 0.7 cd/A in a double-layer device with structure of (ITO/TPD/OPV/Al/Ag). However, with an addition of a LiF layer as an electron-injection enhancing layer, the EL efficiency increases up to 2.3 cd/A with a maximum brightness of 600 cd/m^2. On the other hand, the external EL efficiency of the polyalkyleneoxy disubstituted OPV-based device only reaches 0.2 cd/A in a double-layer device and increases to 0.5 cd/A with an insertion of a LiF layer.[31] Even though both of the oligomers exhibit similar fluorescence quantum yields, because of the electron-withdrawing nature of hexylsulfonyl functionality, **1** has a comparatively lower LUMO level than the polyalkyleneoxy disubstituted OPV. As a result, the better device performance is attributed to a better balance of charge injection/transport properties in the **1**-based OLED. To our surprise, a **2**-based LED was relatively unstable with the EL efficiency of 0.15 cd/A in a three-layer device (ITO/NPD/OPV/PBD/Al).

In contrast, an LED based on **3** as an emissive layer exhibits very low light emission efficiency and short device lifetime. However, the **3**-based device exhibits a clear increase in reverse current upon an increase in illumination, indicating an occurrence of photovoltaic effect (Figure 1). The open circuit voltage, V_{oc}, reaches 1.6 V under the illumination of two Matsushita F15T8/CW fluorescent lamps that have an emission line at 436 nm with an optical power density of ~1 μW/cm^2 at the sample surface. Importantly, no such effect (or negligibly small) was observed in other donor−acceptor OPV-based devices.

To probe the structure−photovoltaic property relationships such as chain length and wavelength responsivity for the polyalkyleneoxy-nitro disubstituted OPV series, 4,4′-polyalkyleneoxy-nitro disubstituted stilbene **4** and four-phenyl-ring OPV **5** were also synthesized (Scheme 2). In view of the electronic absorption spectra of **3**−**5**, there is a progressive increase in both the absorption maximum and extinction coefficient with an

(31) Some of the results were communicated previously: (a) Tao, Y.; Donat-Bouillud, A.; D'Iorio, M.; Lam, J.; Gorjanc, T. C.; Py, C.; Wong, M. S. *Synth. Met.* **2000**, *111*−*112*, 417−200. (b) Tao, Y.; Donat-Bouillud, A.; D'Iorio, M.; Lam, J.; Gorjanc, T. C.; Py, C.; Wong, M. S.; Li, Z. H. *Thin Solid Films* **2000**, *363*, 298−301.

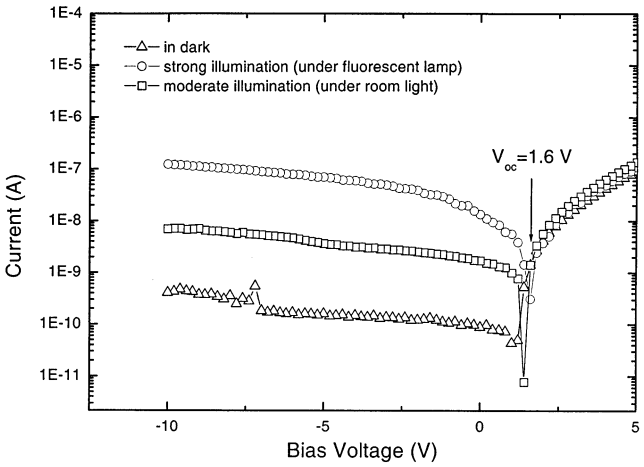

Figure 1. Current−voltage characteristics of the **3**-based device.

Table 1. Summaries of Physical Measurements of Donor−Acceptor OPVs, 1−5, and Results of PM3 Semiempirical Calculations of the Corresponding Methoxy-Acceptor OPVs

molecule	λ_{max}[a] (nm) [ϵ_{max} ($\times 10^4$ M^{-1} cm^{-1})]	fluorescence quantum yield[a]	EL_{max}[b] (nm)	calcd first excited-state dipole moment[c] (D)	calcd ground-state dipole moment[c] (D)
1	375 (5.97)	0.64	520	7.81	6.73
2	375 (5.72)	0.52	535	8.03	5.00
3	401 (4.08)	0.02		9.28	7.21
4	380 (2.75)	0.01		8.95	6.82
5	410 (7.21)	0.04		9.14	7.44

[a] Measurements were performed in $CHCl_3$. [b] The emission maximum in the electroluminescence spectrum of OLED. [c] The dipole moments were calculated by PM3 semiempirical quantum mechanical calculations.

extension of chain length in the homologous series (Table 1). They also show moderate positive solvatochromism (Δ = 14−15 nm from dioxane to DMSO), suggesting the relatively polar excited states. The PM3 semiempirical quantum mechanical calculations have shown that the dipole moments of the first excited state of the corresponding methoxy-nitro disubstituted OPVs are larger than those of the ground state (Table 1), which is consistent with the charge-transfer character of the excited state. Indeed, the measured fluorescence quantum yields of the polyalkyleneoxy-nitro disubstituted OPVs are very low (1−4%) in chloroform. Furthermore, the fluorescence quenching was consistently observed in the solid state, suggesting that the absorbed energy was intrinsically channeled away for other photoinitiated processes.

Organic photovoltaic cells using polyalkyleneoxy-nitro disubstituted OPV as an active layer with a device structure of (ITO/TPD/OPV/Al/Ag) were also fabricated and investigated. All the devices fabricated from these oligomers show clear photovoltaic responses. The spectral response correlates well with the absorption characteristics of the corresponding oligomer in which the photocurrent reaches a maximum at the absorption maximum of the oligomer (Figure 2). These results suggest that the photovoltaic effects observed essentially arise from the polyalkyleneoxy-nitro disubstituted OPVs. In addition, the photovoltaic responsivity increases with an extension of chain length in this series (Figure 2). This also implies that the photovoltaic sensitivity and spectral responsivity can be tuned by the spatial extent

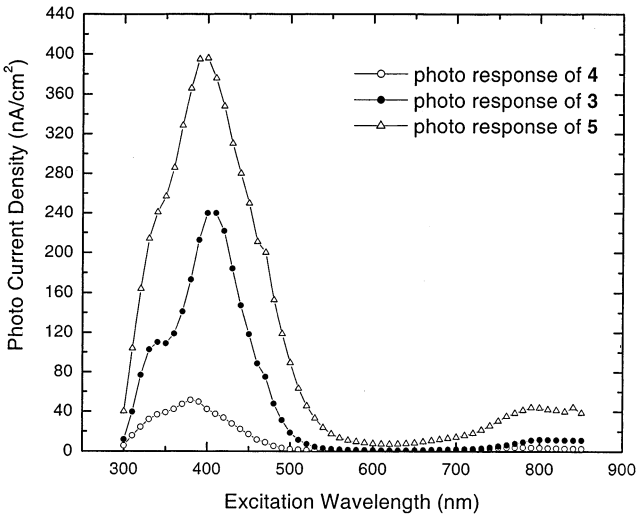

Figure 2. Photocurrent density-wavelength characteristics of the **4**-, **3**-, and **5**-based devices. The excitation power density at 400 nm is about 200 μW/cm^2.

of the π-conjugated chain of these π-conjugated donor−acceptor oligomers. Although the mechanism is not fully understood yet, it is presumed that the strong electron-withdrawing nature of the nitro functionality coupled with the polyalkyleneoxy donor substantially enhances and stabilizes the charge separation process, leading to the fluorescence quenching. The dissociation and migration of charges to the opposite electrodes lead to the photocurrent.

The electronic properties of the electron-donating and electron-withdrawing groups and π-conjugated core are believed to play a crucial role in exhibiting a photovoltaic response as they need to promote an efficient charge separation and dissociation and retard back charge recombination after photoexcitation. To probe and understand the structural factors that can enhance such an effect further, we have synthesized 4-[2-(2-butoxyethoxy)ethoxy]-4′-nitroterphenyl, **17**, and 4-butoxy-4′-nitro disubstituted three-phenyl-ring OPV, **18**. The

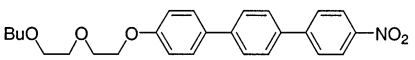

17

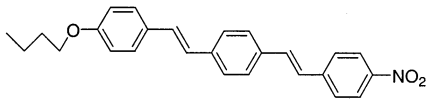

18

importance of the oligophenylenevinylene core for a large photovoltaic effect was put into evidence. With use of an oligophenylene skeleton, such as terphenyl, the photovoltaic response of the **17**-based device drops substantially (Figure 3). This indicates the importance of the conjugation for a charge separation process. In addition, it appears that the chelation property of the ether functionalities in the polyalkeneoxy group does not contribute or is not essential to the photovoltaic effect as the **18**-based device exhibits an even stronger effect (Figure 3).

To improve the device stability, the active photovoltaic layer is fabricated by co-evaporation of Alq_3 and OPV

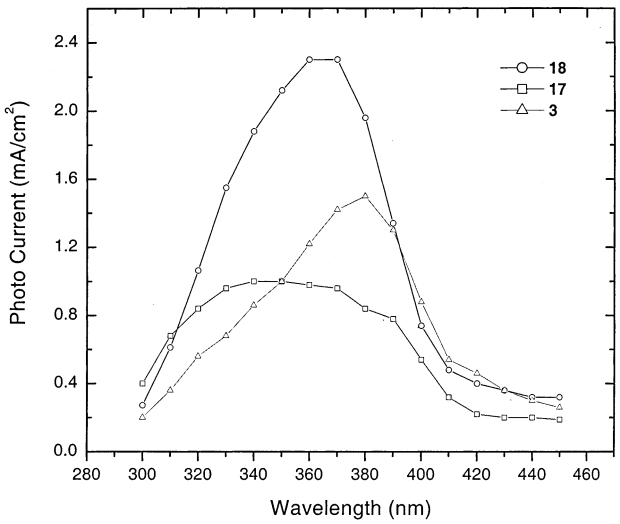

Figure 3. Comparison of the photovoltaic current of the **3**-, **17**-, and **18**-based devices with structure (ITO/TPD/Oligomer/Li/Al) measured under the same light intensity.

at a 100:5 ratio in some devices. The excitation power density at 400 nm is about 200 μW/cm^2, and therefore the responsivity of the **5**-doped device is about 0.002 A/W. The responsivity of the **5**-doped device is approximately 4 times larger than that of the pure Alq_3-based device. These preliminary experiments showed that the responsivity of the **5**-doped devices is about 2 orders of magnitudes lower than those of the state-of-the-art silicon-based photodiodes at 400 nm. We believe that the responsivity can be further improved if lower work function materials are used for the cathode and the layer thickness of each organic layer is optimized. Nevertheless, no further attempt was made to optimize the performance of the devices in this study.

Conclusion

In summary, we have synthesized a novel series of donor−acceptor oligophenylenevinylenes bearing a 2-(2-butoxyethoxy)ethoxy group at one end and an electron-withdrawing group such as alkylsulfonyl, cyano, or nitro group at the other end for various functional properties investigations. 2-(2-Butoxyethoxy)ethoxy-hexylsulfonyl disubstituted OPV-based LED exhibits superior device performance than do LEDs based on the symmetrically 2-(2-butoxyethoxy)ethoxy-disubstituted counterparts. On the other hand, polyalkyleneoxy-nitro disubstituted OPV-based devices exhibit a clear photovoltaic response in which the spectral response of the photovoltaic device corresponds to the absorption characteristics of the oligomer. Furthermore, the photocurrent responsivity increases with an extension of the conjugated length of the oligomer that could provide a means for tuning the spectral response and sensitivity of the photovoltaic device.

Acknowledgment. This work was supported by a Faculty Research Grant (FRG/00-01/II-12) from Hong Kong Baptist University and an Earmarked Research Grant (HKBU2051/01P) from the Research Grants Council, Hong Kong.

CM0208915